Microscopic studies of intercellular infection and protoxylem invasion of tomato roots by Pseudomonas solanacearum

Jacques Vasse, Pascal Frey, André Trigalet

MPMI Vol. 8, No. 2, 1995, pp. 241–251.

Microscopic Studies of Intercellular Infection and Protoxylem Invasion of Tomato Roots by *Pseudomonas solanacearum*

Jacques Vasse, Pascal Frey, and Andre Trigalet

Laboratoire de Biologie Moleculaire des Relations Plantes-Microorganismes, INRA-CNRS, BP 27, 31326, Castanet-Tolosan, Cedex, France

Received 16 May 1994. Accepted 9 December 1994.

The pathogenic interactions between tomato roots and *Pseudomonas solanacearum* were examined microscopically following inoculation with either a pathogenic strain or a nonpathogenic mutant, both harboring a transposon containing a promoterless *Escherichia coli lacZ* gene, which is highly expressed. Several stages were distinguished during tomato root infection by the pathogenic strain. After colonization of exudation sites such as root extremities and axils of secondary roots the bacteria intercellularly infect the inner cortex and the vascular parenchyma. These latter tissues are separated by the endodermis which is not yet fully differentiated at root extremities and is reoriented by the development of lateral roots. Following infection, the pathogenic strain invades protoxylem vessels degrading cell walls. The colonization of approximately 25% of xylem vessels in each vascular bundle of the hypocotyl just above the collar zone is sufficient to induce partial wilting of a tomato plant. In contrast, the nonpathogenic strain was able to infect intercellular spaces of the inner cortex of some secondary roots, but was never observed in the vascular cylinder. The application of this approach should enable the characterization of the process of tomato root infection by genetically defined mutant strains of *Pseudomonas solanacearum*.

Additional keywords: bacterial wilt.

Bacterial wilt caused by *Pseudomonas solanacearum* E. F. Smith is one of the most important diseases of plants, several hundred species being affected (Buddenhagen and Kelman 1964; Hayward 1991). This soilborne bacterium invades root systems, causing rapid wilting of the host plants as the result of heavy colonization and multiplication in vascular tissues. Despite numerous studies devoted to the wilting caused by *P. solanacearum* (Kelman 1953; Buddenhagen and Kelman 1964; Buddenhagen 1986; Hayward 1991), the spatio-temporal stages of the interactions between this vascular pathogen and plants are still poorly understood (Sequeira 1993). In particular, information concerning the process of root infection and the early stages of vascular colonization are fragmentary and mainly based on electron microscopic observations. It is generally accepted that the "points of origin of secondary roots" are the sites through which *P. solanacearum* infects unwounded roots (Schmit 1978), and subsequently progresses towards xylem vessels. In plants inoculated by root immersion after excision of the main root extremity, it has been reported that bacteria invade small cells, adjacent to xylem cells, and that the release of bacteria occurs from infected tyloses which protrude into the large xylem vessels (Wallis and Truter 1978). The process of infection of sectioned tomato petioles by *P. solanacearum* has also been described (Petrolini et al. 1986). In this case, bacterial adhesion to xylem vessel cell walls is followed by degradation of these cell walls and by the formation of tyloses in uninvaded vessels. Subsequent bacterial multiplication is accompanied by the breakdown of vessels and the development of large cavities filled with cell debris and bacteria. Agrios (1988) reported that the formation of such lysogeneous cavities is a general feature of bacterial pathogens that cause vascular wilts.

Recently, cytological studies of plant-microbe interactions have been facilitated by the use of genetically modified microoganisms harboring gene fusions with the promotor of a gene which is expressed constitutively. For example, the symbiotic interactions between alfalfa and *Rhizobium meliloti* have been studied with bacterial strains carrying *Escherichia coli lacZ* reporter gene fusions (Boivin et al. 1990; Vasse et al. 1993; Ardourel et al. 1994). Using the same method, it has also been shown that a novel plant-defense gene in tobacco is specifically activated after inoculation with strains of *P. solanacearum* able to induce a hypersensitive response (Pontier et al. 1994).

In this paper, we report on microscopic studies of infection of tomato roots by two strains of *P. solanacearum* which carry *E. coli lacZ* reporter gene fusions. The objectives of this work were to compare the temporal and spatial patterns of infection and colonization of the pathogenic strain GMI1485 with those of the spontaneous nonpathogenic strain GMI2550.

RESULTS

The root infection process and vascular colonization by the pathogenic strain.

The interactions between tomato roots and the pathogenic strain GMI1485 have been studied on whole root systems sampled at different times after inoculation and compared to uninfected roots. The histological localization of bacteria in

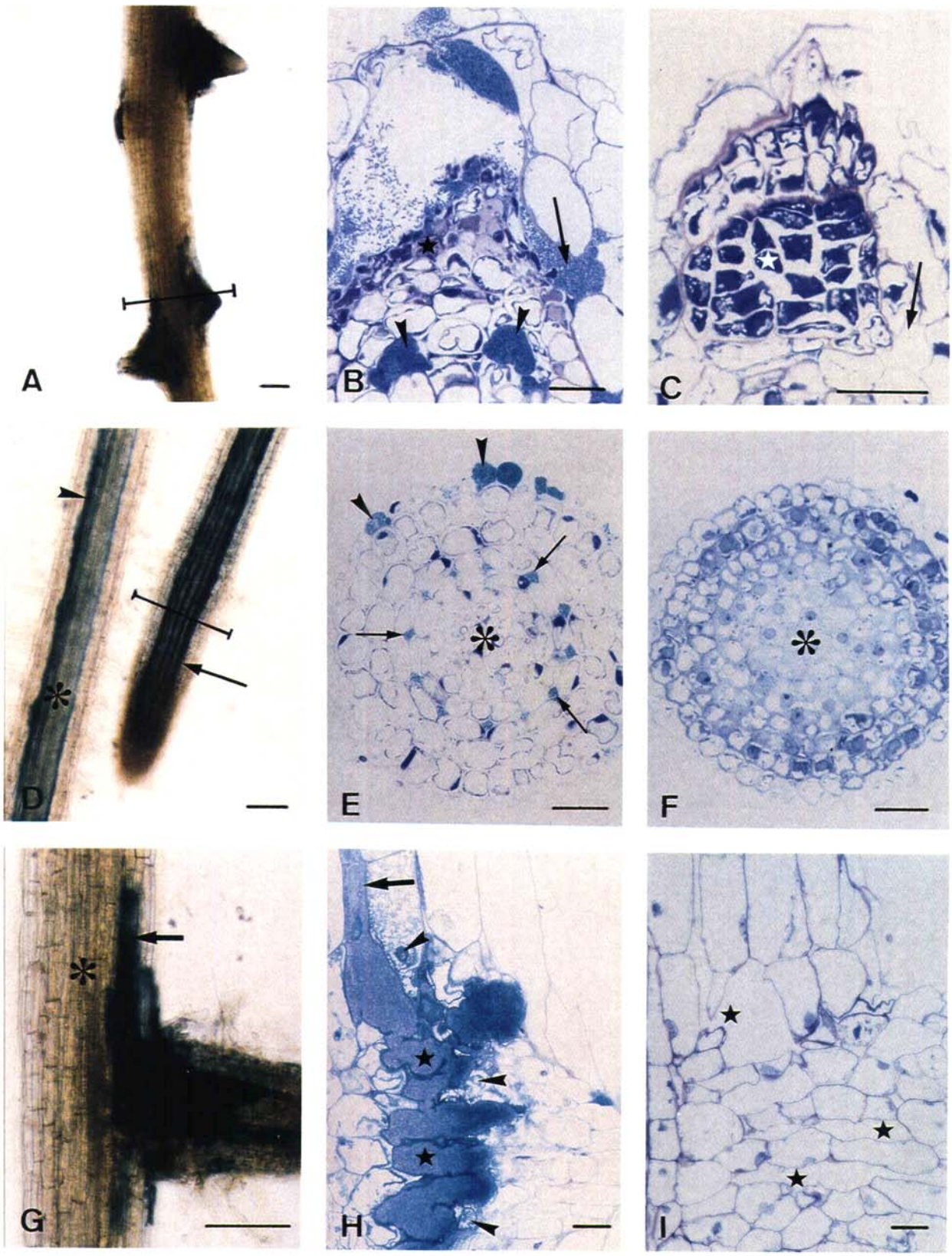
A
B
C
D
E
F
G
H
I

tomato plant tissue was observed by light microscopy, after staining of the bacterial β-galactosidase activity which formed a dark blue precipitate in the presence of the chromogenic substrate X-Gal. This spatio-temporal microscopic study has permitted different stages of the interaction to be distinguished.

One day after inoculation of plants cultivated in liquid medium, the bacteria were found to colonize mainly the surface of root extremities, particularly the longitudinal grooves observed between the epidermal cells at the surface of the root elongation zone (data not shown). Compared to uninoculated roots, the elongation zone was often shortened, while the adjacent zone, where root hairs develop, was swollen. Following inoculation, root extremities were the earliest sites colonized. However, the intercellular cortical spaces at the emergence site of secondary roots were also rapidly colonized (Fig. 1A). Sections of colonized and uninoculated root sites from control plants where lateral roots emerged showed that bacteria were mainly located in the intercellular spaces of the inner cortex and that in the case of colonization the meristematic cells of the emerging lateral roots underwent necrosis (compare Fig. 1B and C). The intercellular spaces at the axils of lateral roots which had developed prior to inoculation, in the oldest part of primary roots, as well as neighboring individual epidermal cells, were colonized later. It is worth noting that the meristems of such developed lateral roots did not display necrotic features following inoculation (data not shown).

Surface colonization was followed by cortical infection, the second stage of the pathogenic interaction. Cortical infection was observed 2 to 3 days after inoculation, first at root extremities and later at the axils of secondary roots. Transverse sections of root extremities exhibiting inner longitudinal and parallel blue lines (Fig. 1D), showed that most of the intercellular spaces next to the central cylinder were infected and that some epidermal cells were filled with bacteria (Fig. 1E). Detailed observations of sections of uninoculated root extremities indicated that intercellular spaces had not developed in the cortex and that xylem vessels and the endodermis had not yet fully differentiated at this root level (Fig. 1F). Deep infection was also noticed in the cortex of the primary root located in the area where secondary roots had developed (Fig. 1G). Sections at this second infection site revealed bacteria forming large and confluent intercellular pockets located at the inner cortex level and showed that the cortical cells next to the infection pockets presented features of degeneration (Fig. 1H). This later observation has been confirmed at the ultrastructural level by transmission electron miscroscopy (data not shown). In contrast, no cell degeneration was observed on sections of secondary root axils of uninoculated plants, even if large intercellular spaces developed in the cortex at this root site (Fig. 1I).

The third stage of the interaction is characterized by stele infection and xylem invasion. Both vascular cylinder infection and xylem penetration were seen as soon as 3 days after inoculation. At this time, the observation of whole roots indicated that bacteria had progressed from infection sites towards inner tissues and had infected some xylem vessels. Such features first occurred in parts of developed secondary roots (Fig. 2A). Transverse sections of these root segments were compared to similar sections of uninoculated secondary root segments, and this revealed that bacteria had infected the intercellular spaces of the vascular parenchyma located in the vicinity of a protoxylem vessel which was also generally invaded (compare Fig. 2B and C). In secondary roots showing a stronger infection, the xylem vessels adjacent to the protoxylem were also invaded and, the surrounding parenchyma cells were highly degraded (data not shown).

Approximately 1 week after inoculation, the axils of some secondary roots which had developed in the older part of the primary root were highly infected. At these sites a heavy infection as deduced from a dark blue staining prevented the cortex being distinguished from the central cylinder. However, the fact that epidermal and cortical cell layers on the other side of the root axil remained unstained suggested that these tissues had not been infected (Fig. 2D). Transverse sections of primary root segments adjacent to heavily infected root axils showed that bacteria had infected most of the intercellular spaces of both the inner cortex and the vascular parenchyma next to the outer protoxylem vessels. These two types of infected spaces were not confluent and were separated by the endodermis. Many parenchyma cells, adjacent to infected intercellular spaces, displayed signs of degeneration (Fig. 2E). In transverse sections of primary roots from uninoculated control plants, the endodermis was easier to distinguish and no signs of cell degeneration were observed (Fig. 2F).

Ultrastructural studies of infected secondary root axils revealed that the cell walls of xylem vessels were modified as a result of pathogen infection. In several xylem vessels, located at the vascular junction between primary and secondary roots, a multilayered coating was observed all over the cell walls,

Fig. 1. Light microscopy of root cortex infection of tomato by *Pseudomonas solanacearum* strain GMI1485. Bacteria were localized by histochemical staining of β-galactosidase activity in whole roots (**A, D,** and **G**) in semithin section (**B, E,** and **H**). Semithin sections of control, uninoculated plants are included (**C, F, I**). All semithin sections were poststained with toluidine blue. **A,** Colonization of the emergence sites of secondary roots, 1 day after inoculation. **B,** Section at a root emergence site, as indicated in A. Bacterial infection (arrow) in a cortical space at root emergence. Two intercellular bacterial pockets (arrowheads) and necrotic meristematic cells (black star) are seen. **C,** Section at root emergence site of an uninoculated plant. Cortical spaces are observed (arrow) near healthy meristematic cells (white star). **D,** Right, infection (arrow) at the tip of a secondary root. Left, in another secondary root, bacteria (arrowhead) are localized in tissues adjacent to the vascular cylinder (asterisk). **E,** Transverse section of an infected root extremity, as indicated in D. Colonization of epidermal cells (arrowheads) and intercellular infection of inner cortex (arrows) are observed. The surrounding the central cylinder (asterisk), the endodermis has not yet completely differentiated. **F,** Transverse section of an uninoculated root extremity. The central cylinder (asterisk) has not differentiated and intercellular spaces were not observed at this root level. **G,** Progression along the vascular cylinder (asterisk) of cortical infection (arrow) at the axil of a secondary root, 4 days after inoculation. **H,** Tangential section of an infected secondary root axil showing confluent and intercellular infection pockets of bacteria (stars). The arrow points to an infected intercellular space of the inner cortex cell layers in the primary root while arrowheads indicate degenerating cortical cells. **I,** Tangential section of an uninoculated secondary root axil. Large and confluent cortical intercellular spaces (stars) were noticed at this root level whatever the sample. Scale bars = 100 μm (**A, D,** and **G**), 25 μm (**B, C, E, F, H,** and **I**).

including secondary wall lignin appositions (Fig. 3A). No invasion of such wall-coated vessels was observed, despite the fact that bacteria were localized both in intercellular spaces and in degenerated parenchyma cells adjacent to them. In contrast, bacteria were able to degrade the cell walls of uncoated xylem vessels. At this stage, degradation only affected the primary cell wall between secondary wall appositions, allowing some bacteria to penetrate into uninvaded xylem vessels (Fig. 3B). Subsequently, the lumens of xylem vessels were colonized by actively multiplying bacteria. The colonized xylem vessels were filled with an extracellular fibrillar and vesicular material, except for an electronically empty halo surrounding each bacterium (Fig. 3C). When compared to the cell wall of uninvaded xylem vessels, the cell wall of a colonized vessel appeared to be extensively degraded (compare Fig. 3D and E). Fragments of the degraded cell wall obviously appeared to be part of the extracellular material which filled all the colonized vessels (Fig. 3D).

Ten days after inoculation, relatively few plants cultivated in tubes with liquid medium presented signs of wilting while, in general, all tomato plants cultivated and inoculated in pots were either totally or partially wilted. Vascular colonization of

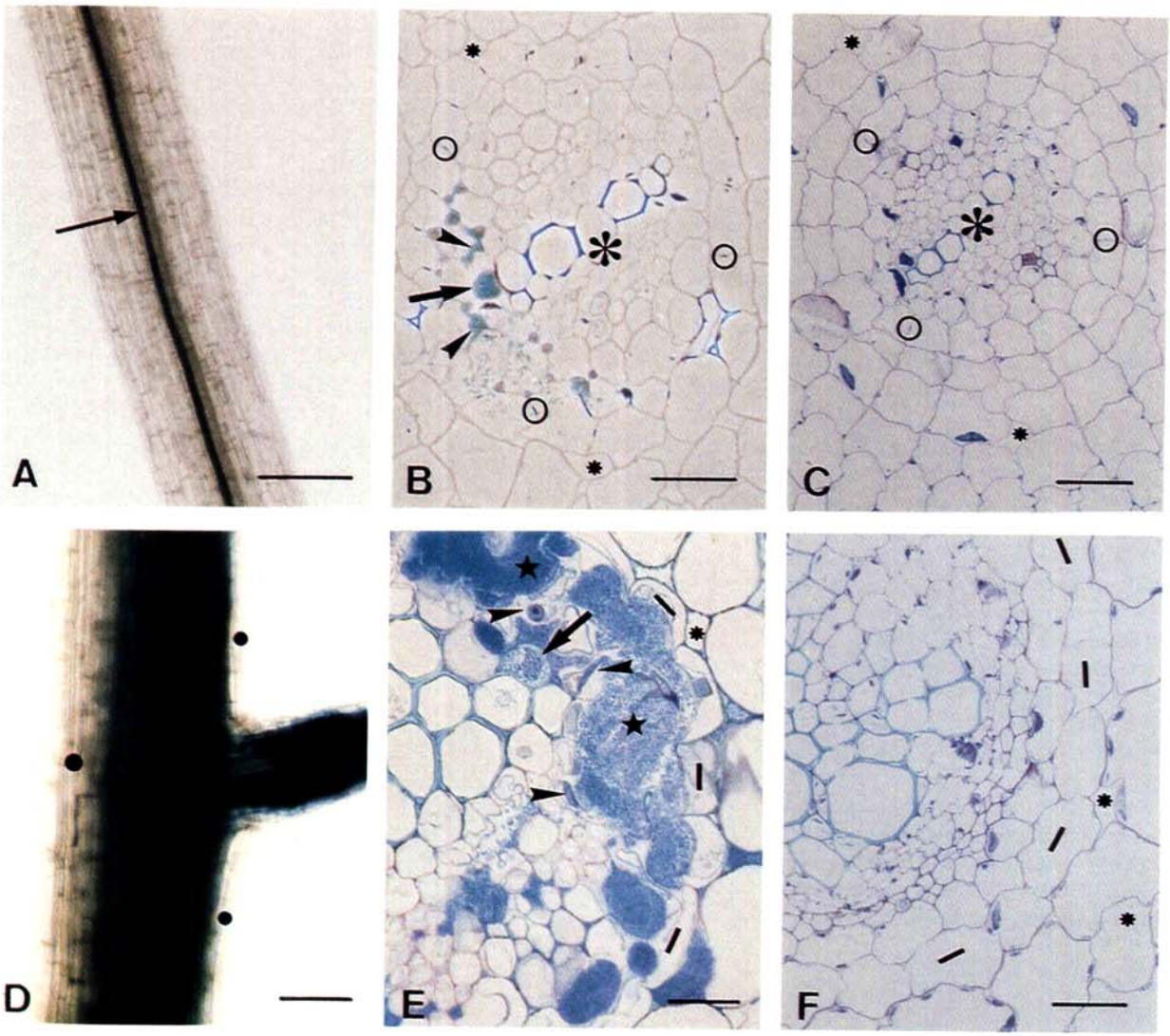

Fig. 2. Light microscopy of central cylinder infection and protoxylem invasion of tomato roots by *P. solanacearum* GMI1485. Bacteria were localized by histochemical staining of β-galactosidase activity in whole roots (**A** and **D**) and in semithin sections (**B** and **E**). Semithin sections of control, uninoculated plants are included (**C** and **F**). Semithin sections were poststained with toluidine blue, except B. **A,** Bacteria (arrow) are observed in a vascular element of a secondary root 3 days after inoculation. **B,** Detail of a transverse section of a secondary root, observed by phase contrast and showing the infection in one side of the stele. Bacteria are localized in the intercellular spaces of the vascular parenchyma (arrowheads) and in a protoxylem vessel (arrow). In B and C, equivalent section as B of an uninoculated plant. In B and C, circles highlight the Caspary strips of the endodermis surrounding the vascular cylinder (asterisk) and intercellular spaces (small asterisks) were only observed in the cortex. **D,** Infection at the axil of a secondary root which has developed in the upper part of a primary root, 6 days after inoculation. Black dots show root tissues that remain uninfected. **E,** Detail of a transverse section of an infected primary root, next to infected secondary root axil. Cortical and central cylinder intercellular spaces are infected but are separated by the endodermis which is not disrupted (dashes). Large intercellular bacterial (stars) and degraded xylem parenchyma cells (arrowheads) are observed in the vicinity of an uninvaded outer xylem vessel (arrow). As in B, C, and F, intercellular spaces (small asterisks) were observed in the inner cortex. **F,** Part of a transverse section of a primary root proximal to the axil of a developed secondary root from an uninoculated plant. No cell degradation is observed and the endodermis (dashes) is easier to distinguish than in E. Scale bars = 100 μm (**A** and **D**), 25 μm (**B, C, E,** and **F**).

partially wilted plants was studied at four different levels of the plant axis. The first level corresponded to the upper part of the main root, where most of the secondary roots develop. At this level, 20% of the xylem vessels, seen as one cluster in the stele, appeared colonized (Fig. 4A). The second level examined, the lowest part of the hypocotyl, is a root zone which normally lies in the ground and from which numerous adventitious roots develop. At this level, the vascular tissues had differentiated into four distinct bundles; about 25% of the vessels of each bundle were colonized, while others remained uninvaded (Fig. 4B). At the third level, the middle part of the hypocotyl, some vessels of the primary xylem appeared colonized, but numerous vessels remained free of bacteria (Fig. 4C). Finally, in the epicotyl, the fourth level observed, small and large bundles alternated at the periphery of the stele. Bacteria were observed only in a few xylem vessels of the large bundles, in the vicinity of which brownish cells were clearly detected (Fig. 4D).

Root infection by the nonpathogenic mutant.

The capacity of the nonpathogenic mutant GMI2550 to infect tomato plants was compared to that of the pathogenic strain described above. None of the plants grown and inoculated in pots exhibited wilt symptoms, even 15 days after

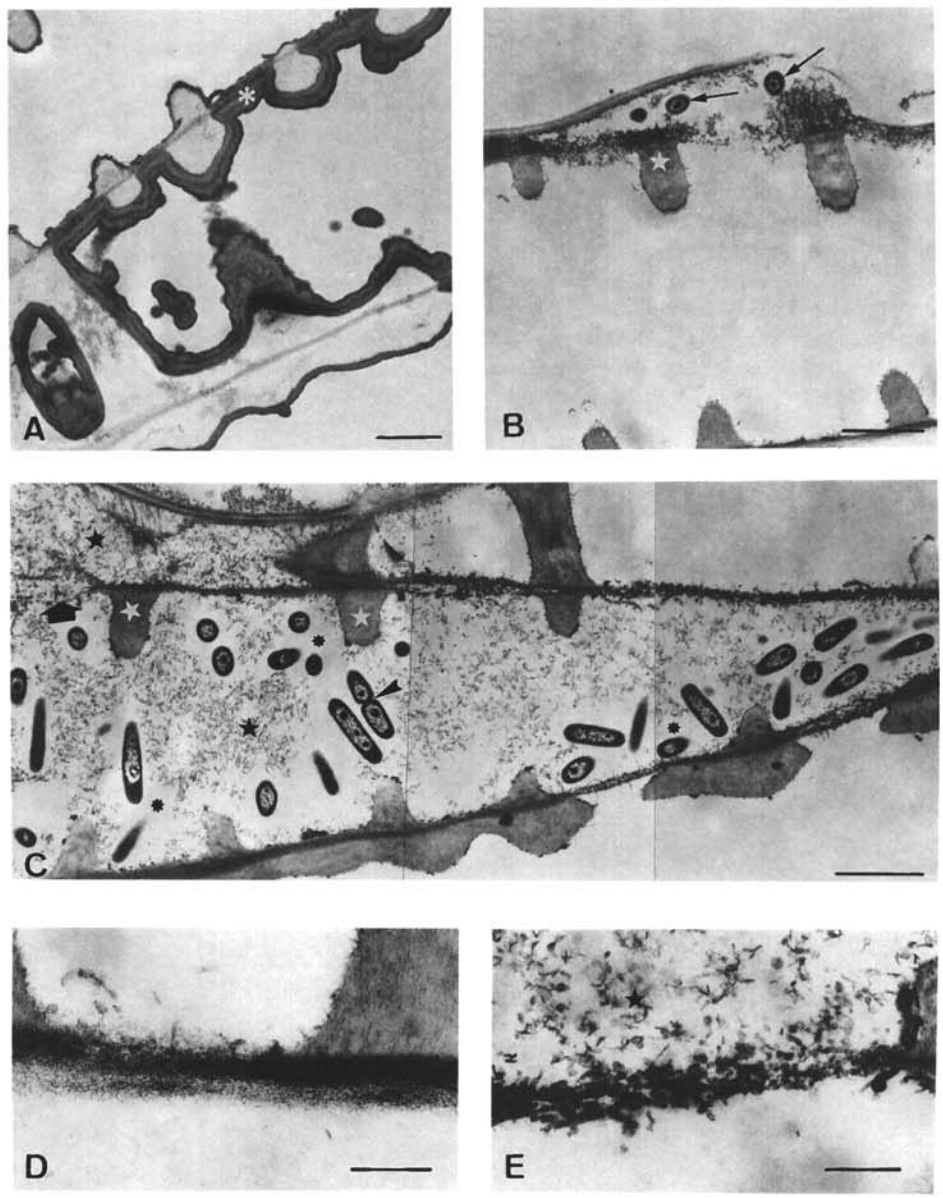

Fig. 3. Electron microscopy of bacterial penetration into xylem vessels of primary roots. **A,** Wall coating in uninvaded xylem vessels (white asterisk). Note the multilayer composition of the coating material. **B,** Bacteria (arrows) inserted in the degraded primary cell wall of a xylem vessel. The secondary cell wall appositions of the xylem vessel are not degraded (white star). **C,** Part of an invaded xylem vessel. Bacteria are separated from an extracellular material (black stars) by an electronically empty halo (black asterisks). The arrowhead points to a dividing bacterium. The degradation of a primary cell wall of the infected xylem vessel (left upper corner of the micrograph, large arrow) and undegraded secondary cell wall appositions (white stars) are seen. **D,** Cell wall of an uninvaded xylem vessel. **E,** Degraded primary cell wall of an invaded xylem vessel containing extracellular material (black star). Scale bars = 2 µm (**A, B,** and **C**), 0.5 µm (**D** and **E**).

inoculation. Light microscopy images of transverse slices made in the upper part of the main root or in the lower part of the hypocotyl, the first and the second levels, respectively, described above, showed that xylem vessels appeared to be uninvaded (Fig. 5A). The absence of observed nonpathogenic bacteria in any of the plants tested suggested that this mutant strain was either unable to colonize the vascular system of tomato or was invasive at an undetectable level. Root infection by this mutant was studied by observing whole root systems of plants grown and inoculated in liquid conditions. When compared to the pathogenic strain, which preferentially occupied the longitudinal intercellular spaces of root extremities, nonpathogenic bacteria colonized fewer numbers of root extremities and generally formed aggregates at the root surface. No bacterial infection of the inner intercellular spaces at root extremities was observed (data not shown).

One week after inoculation, the axils of some developed lateral roots in the older part of primary roots were colonized by aggregated mutant bacteria, which also accumulated in a few individual epidermal cells (Fig. 5B). Sections of colonized lateral root axils indicated that intercellular infection was restricted to the outermost cortical cell layers, and that even 2 weeks after inoculation, the nonpathogenic bacteria were seen neither at the inner cortex level nor in the stele of primary and secondary roots (Fig. 5C). Nevertheless, we noticed that parts of some secondary roots could be infected (Fig. 5D). Transverse sections of such root segments revealed an intercellular infection, with large and confluent bacterial pockets surrounding the endodermis (Fig. 5E). However, despite thorough observations of a large number of sections, the infection of the vascular tissues was never observed.

DISCUSSION

Significant microscopic studies of plant-microbe interactions, including those involving vascular pathogens, depend to a large part on the methods used to localize the microorganism at different stages of the interactions. The capacity to visualize enzyme production by a simple histochemical staining procedure (Teeri et al. 1989), and therefore to be able in planta to accurately localize genetically modified microorganism harboring marker genes, has so far proved to be unrivaled in deciphering the spatio-temporal relationships which are established between a plant and its microbial partner (Couteaudier et al. 1993).

Using strains which highly express a gene fusion, we have cytologically investigated tomato root infection and colonization by *P. solanacearum* and have shown that different stages of the plant-bacteria interaction can be distinguished. These are discussed below.

Two colonization sites exist on the root surface.

Early interaction between *P. solanacearum* and tomato roots results in the surface colonization of two precise root sites, namely the elongation zone and the axils of emerging or developed secondary roots. The elongation zone is the major

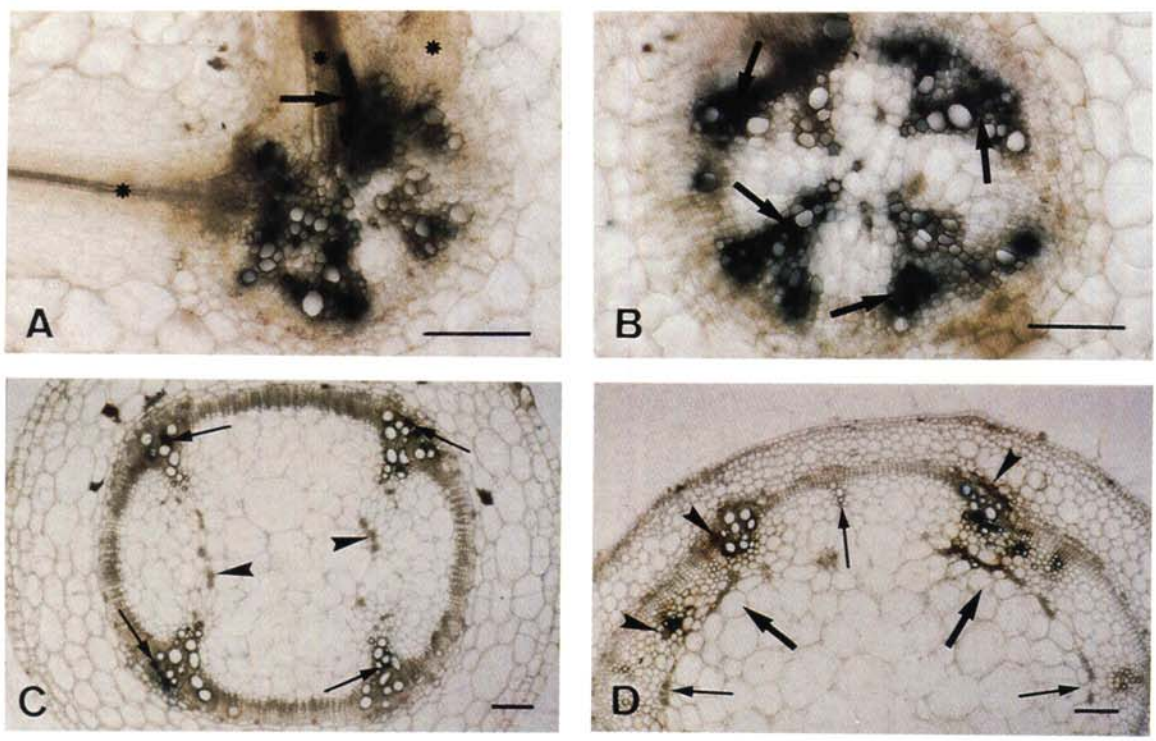

Fig. 4. Vascular colonization at different levels of a partially wilted plant. Transverse slices obtained from the same plant after histochemical staining of β-galactosidase activity in planta. **A,** Upper part of the main root. Approximately 20% of the xylem vessels are colonized. An invaded xylem vessel (arrow) is observed at the base of one of the three secondary roots (asterisks). **B,** Lowest part of the hypocotyl near to the collar zone. The stele shows four distinct vascular bundles, each containing numerous colonized vessels (arrows). **C,** Aerial part of the hypocotyl with inner phloem (arrowheads) observed in the pith. The four bundles of primary xylem show colonized vessels (arrows). **D,** Epicotyl. Bacterial colonization is seen in the large vascular bundles (thick arrows) but not in the alternating small bundles (thin arrows). Brownish cells (arrowheads) are observed in the vicinity of invaded bundles. Scale bars = 250 μm.

zone of plant root exudation and is commonly colonized by numerous microorganisms of the rhizosphere (Rovira 1973; Forster 1986). Thus, the colonization of the root elongation zone and the swelling of the adjacent root hair zone within the 2 days following inoculation of tomato plants with *P. solanacearum*, are not specific to this interaction and have already been reported following tomato root inoculation with *Azospirillum brasilense* (Hadas and Okon 1987). However, elongation zones were very rapidly colonized by *P. solanacearum*. Our studies show that some individual epidermal cells in the vicinity of the axil of lateral roots are also colonized. It seems likely that the colonization by *P. solanacearum* which occurs at exudation sites along the root system is the result of a trophic chemotaxis by the microorganism.

The infection process of the root cortex is intercellular.

Intercellular infection of the innermost cortical cell layer occurs at the sites previously colonized, i.e., root extremities and axils of developed lateral roots, and is observed as longitudinal infection adjacent to the vascular cylinder. The formation of files of intercellular bacteria at root extremities is likely to take place with plant growth and with bacterial development at the level of the inner cortex. Despite thorough observations of transverse sections, we have not been able to observe bacteria passing through the cortical cell layers of root extremities and the way in which bacteria migrate from the colonization site to the inner cortex is not known. Infection of intercellular spaces of the inner cortex at axils of secondary roots might occur through the natural wounding of the cortex, which results from lateral root development.

The formation of intercellular spaces is enhanced in tomato roots when plants are cultivated in flooded conditions (Yu et al. 1969). Our cytological observations of root sections from uninoculated control plants demonstrate that intercellular spaces were mainly present in the root cortex except at root extremities. Consequently, it seems that infection of intercellular spaces of tomato root cortex could be favored when plants are cultivated in liquid medium. Such a hypothesis might explain why the development of bacterial wilt induced by *P. solanacearum* is increased in tropical areas character-

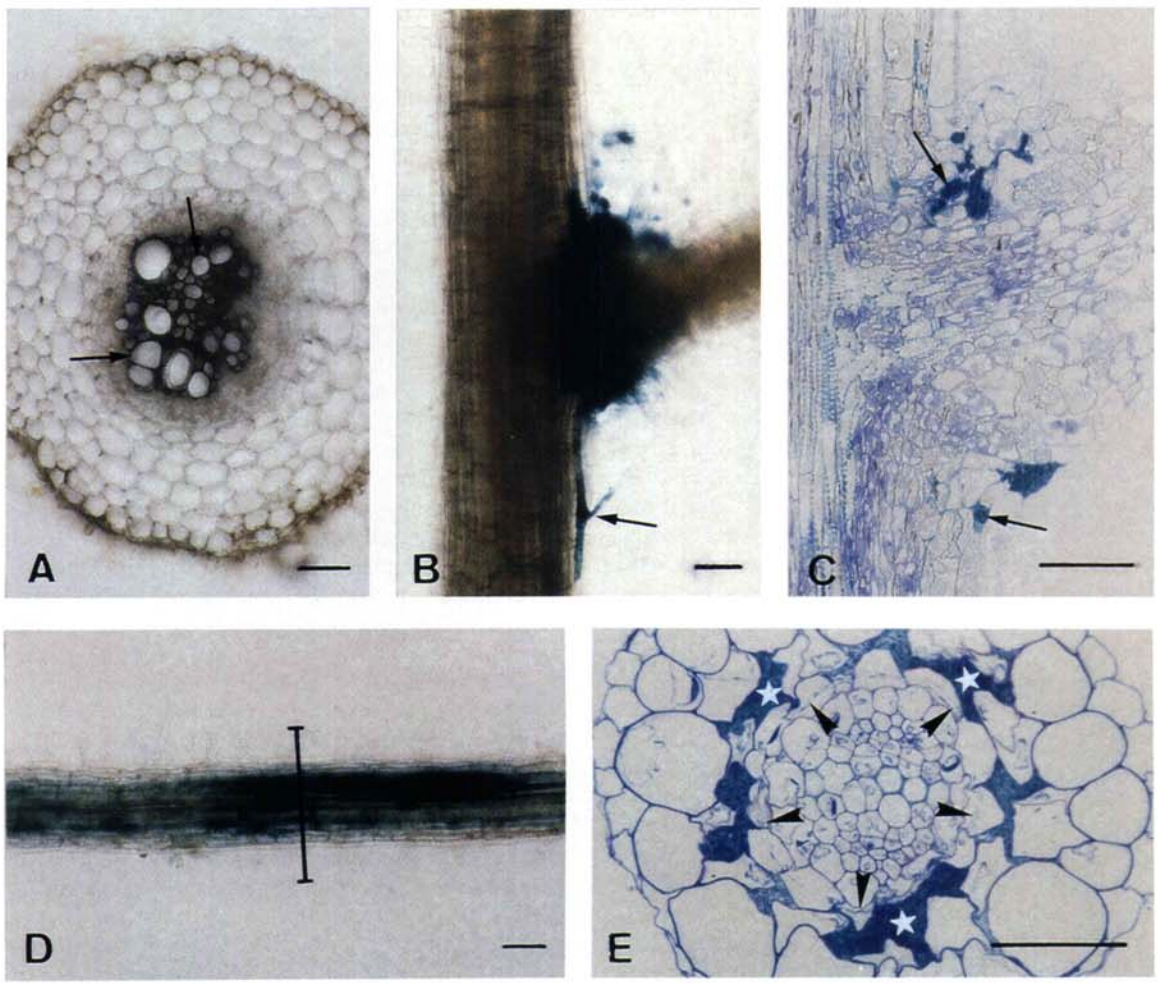

Fig. 5. Tomato root infection by the spontaneous nonpathogenic P*seudomonas solanacearum* mutant GMI2550. Bacteria were localized by histochemical staining of β-galactosidase activity in whole root (**A, B,** and **D**) and root sections (**C** and **E**). Semithin sections were poststained with toluidine blue. **A,** Transverse slice in upper part of the main root of a symptomless plant 15 days after inoculation by the mutant strain. None of the xylem vessels (arrows) appear to be colonized. **B,** Bacterial colonization at a secondary root axil and in an epidermal cell (arrow), 10 days after inoculation. **C,** Longitudinal section of a secondary root axil. Limited intercellular infection (arrows) of the primary root cortex. **D,** Cortical infection of part of a secondary root, 4 to 5 days after inoculation. **E,** Transverse section of an infected secondary root part as indicated in D. Bacteria are seen in intercellular pockets (white stars) in the innermost root cortex. Arrowheads point to the endodermis layer. Scale bars = 100 µm (**A, B, C,** and **D**), 50 µm (**E**).

ized by high soil moisture contents (Buddenhagen and Kelman 1964).

Is the endodermis a natural barrier to vascular cylinder penetration?

The intercellular infection which is first seen in the inner cortex is then observed in the vascular parenchyma adjacent to xylem vessels. Histologically, these two tissues are separated by the endodermis, which has never been observed interrupted in control plants or infected by the pathogen. These results strongly suggest that this particular cell layer might resist a transversal progression of the pathogen from the cortex to vascular tissues. Our observations agree with previous data, indicating that the endodermis, with its suberized radial walls and stored phenolic compounds, forms a barrier to invasion of tomato vascular tissues by the pathogen *Fusarium oxysporum* f. sp. *lycopersici* (Beckman 1987). Thus, to reach the vascular cylinder, *P. solanacearum* must take the opportunity of root sites where the physical endodermal barrier is either not yet fully differentiated at root extremities, or is reoriented at secondary root axil by the outgrowth and the development of lateral root. It is important to notice that these two potential sites of vascular cylinder infection are also preferential sites of root exudation which are colonized by the microorganism.

Invasion of the protoxylem occurs via vessel wall degradation.

The invasion of some protoxylem vessels is the stage following the infection of plant tissues. This stage occurs more frequently and seems to be more efficient at the bases of secondary root than at root extremities. Moreover, the precise site where the pathogen first penetrates into protoxylem vessels along the secondary root is difficult to locate with accuracy. Consequently, xylem invasion was studied preferentially at infected lateral root axils by electron microscopy. The cell wall coating of xylem vessels at the vascular junction between main roots and developed secondary roots was noticed during this study and related to development of bacterial infection pockets in vascular parenchyma. Electron-opaque material coating vessel walls has also been reported in wilt diseases caused by the pathogenic fungi *Fusarium oxysporum* and *Verticillium albo-atrum* on various plants (Bishop and Cooper 1983; Shi et al. 1992). According to Street et al. (1986), this coating material seems to be composed of suberin or ligninlike material. It has been suggested that cell wall coating could act as a physical barrier to xylem invasion by pathgenic fungi (Robb et al. 1987; Shi et al. 1992). The fact that coated xylem vessels were never observed to contain bacteria strongly suggests that coating may also be a physical barrier to *P. solanacearum* penetration into tomato xylem vessels.

In the vicinity of the vascular junction, we have observed some bacteria inserted into partially degraded primary cell walls of xylem vessels, while other vessels were completely invaded and displayed advanced signs of cell wall degradation with the exception of lignin appositions. It is worth noting that *P. solanacearum* produces extracellular endoglucanase, endo- and exo-pectinases (Schell 1987; Allen et al. 1993) able to degrade primary and secondary plant cell wall components. These enzymes are considered as important factors of virulence (Schell et al. 1988; Denny et al. 199(Kang et al. 1994). A material, which could be partly derive from the degradation of vessel cell walls, appeared to fill th infected vessels where bacteria continued to multiply. Degra dation of primary cell walls of invaded xylem vessels has als been reported in cabbage leaves and tomato stems infected b the vascular pathogenic bacteria *Xanthomonas campestris* p' *campestris* and *Clavibacter michiganensis* spp. *michiganesi* respectively (Wallis et al. 1973; Wallis 1977). In these stuc ies, cell wall degradation was noticed in aerial parts of ir fected plants and in advanced stages of pathogenesis. Ou results show that the same type of phenomenon occurs at th root level and during the early stages of the interaction be tween *P. solanacearum* and tomato.

Colonization of a few xylem vessels is sufficient to induce wilting.

Bacterial colonization of all xylem vessels was never ob served, whatever the level studied between the main root an(the epicotyl of partially wilted plants. However, all vascula bundles contained invaded vessels, with the exception of th(alternating small bundles in the epicotyl. The largest percent age of invaded xylem vessels was observed above the colla zone, the plant level which is characterized by a histologica organization of vascular tissue between the root and the aeria part. At this level, a maximum of 25% of xylem vessels wa: colonized in each of the four vascular bundles observed. Ever if this percentage is probably underestimated, due to the pas sive discharge of bacteria from vessels during experimenta procedures, it seems likely that the colonization of less thar half of the xylem vessels is sufficient to provoke a partia impairment of the water flow at the collar zone, which probably induces the symptoms of wilting.

The nonpathogenic mutant is partially infective but not invasive.

The mutation which affects the nonpathogenic strain GMI2550 is spontaneous, not genetically defined, and pleotropic. It results in reduced exopolysaccaride production, endoglucanase activity, and virulence, while it causes increased polygalacturonase activity (Trigalet, Arlat, and Vasse, unpublished results). The process that coordinately affects these traits has been termed phenotype conversion (PC) and the resulting mutants as PC types (Brumbley and Denny 1990). Furthermore, it has been demonstrated that a mutation in the *phcA* gene of the wild-type strain AW1 induces phenotype conversion (Brumbley and Denny 1990). It has also been described that spontaneous nonpathogenic mutants of *P. solanacearum*, which are impaired in exopolysaccharide production, are sensitive to agglutination by divalent cations and are fixed onto cell walls by Solanaceae agglutinins (Duvick and Sequeira 1984; Young and Sequeira 1986). The mutant strain GMI 2550 quickly auto-agglutinates in the presence of 20 mM $CaCl_2$ or of tomato crude lectin (Trigalet, unpublished results). The penetration of GMI2550 into inner root tissues seems to be prevented by external fixing and clumping, even if this strain produces higher polygalacturonase activity than the wild-type strain GMI1485. Thus, the nonpathogenic mutant GMI2250, which has never been observed reaching vascular parenchyma and xylem vessels, and whose isogenic mutant MR1 has never been reisolated from aerial plant axe

(Trigalet and Trigalet-Demery 1990), can be defined as partially infective, but not invasive.

The stages of the *P. solanacearum*–tomato interactions presented in this paper match with the different phases that characterize the interactions between the vascular pathogens *Verticillium* and *Fusarium* spp. and their appropriate plant hosts (Talboys 1964; Beckman 1987). In these latter interactions, two determinative phases, which are essential for vascular invasion, are followed by an expressive phase during which wilt symptoms are induced (Beckman 1987). The first determinative phase concerns the stages occurring "outside the vascular cylinder" and corresponds to root surface colonization and intercellular cortical infection as described in this study. The second determinative phase refers to pathogen penetration "inside vascular tissues," and is equivalent to both the infection of the vascular parenchyma and the invasion of xylem vessels which we have reported. Finally, the expressive phase as defined by Beckman (1987), is characterized by wilt symptoms and disease development. We propose that this terminology should be slightly modified to differentiate clearly between intercellular infection of plant tissues and intracellular invasion of xylem vessels. Thus, the wild-type strain used in this study is fully infective since it can infect intercellular spaces of both cortical and vascular parenchyma tissues, is invasive since it penetrates into xylem vessels, and is expressive since it rapidly causes wilt disease in a compatible host plant. By comparision, we describe the nonpathogenic strain, which is only able to infect cortical tissues, as partially infective and noninvasive.

It is worth noting that phenotypes of mutant strains of *P. solanacearum* are described currently only with reference to the expressive phase of disease, in terms of virulence or of aggressiveness (Boucher et al. 1992). Our objective is now to take advantage of the present study to investigate cytologically, at the root level, infection and invasion phenotypes of genetically defined mutant strains of *P. solanacearum*, affected in important pathogenicity determinants, such as *hrp* and *eps* genes (Boucher et al. 1987; Denny and Baek 1991).

MATERIALS AND METHODS

Bacterial strains and inoculum preparation.

Strains GMI1485 and GMI2550 of *P. solanacearum* used in this study are derivatives of the wild-type strain GMI1000 (Boucher et al. 1985) and carry insertions of the transposon Tn*5*-B20 containing a promoterless *E. coli lacZ* gene (Simon et al. 1989). The strain GMI1485 has a wild-type pathogenic phenotype on tomato plants and harbors a Tn*5*-B20 gene fusion insertion that maps outside of the *hrp* gene cluster, a region essential for the expression of the *h*ypersensitive *r*esponse on tobacco and *p*athogenicity on tomato (Boucher et al. 1987). GMI1485 expresses the highest β-galactosidase activity of all the Tn5-B20 strains so far tested in MM medium supplemented by glucose (Arlat et al. 1992). The nonpathogenic strain GMI2550 results from the introduction by transformation (Boucher et al. 1986) of the Tn*5*-B20 insertion carried by the pathogenic strain GMI1485 into the nonpathogenic strain GMI2000, also named MR1, which is a spontaneous mutant derivative of the strain GMI1000 (Message et al. 1978; Trigalet and Trigalet-Denny 1990). The mutant strain GMI2000 develops small, butyrous, dark red colonies with a rough aspect on triphenyl tetrazolium chloride agar medium, whereas the pathogenic strain GMI1000 presents larger colonies which are white with a pink center and have a smooth aspect. The strain GMI2000 has a modified lipopolysaccharide and lacks the major fraction of the exopolysaccharides produced by the wild-type strain GMI1000 (Drigues et al. 1985; Orgambide et al. 1991). Moreover, strain GMI2000 induces a hypersensitive response in leaves of tobacco cultivars Samsun and Bottom Special (Message et al. 1978; Boucher et al. 1985).

Enzyme activities of polygalacturonase and endoglucanase in culture supernatants of strains GMI1000, GMI1485, GMI2000, and GMI2550 were tested following a procedure previously described (Arlat 1989).

Bacteria were grown in peptone broth (Boucher et al. 1985) at 30°C for 24 h. The inoculum concentration was about 5×10^8 CFU ml^{-1} for both strains.

Plant growth conditions and root inoculation.

Seeds of *Lycopersicon esculentum* cv. Supermarmande (Vilmorin) were surface-sterilized and germinated as previously described (Boucher et al. 1985). Five germinated seeds were deposited on stainless steel gauze in large sterile test tubes (30 mm diameter, 200 mm long), at the surface of 35 ml of 0.46% (w/v) Murashige and Skoog plant nutrient solution (CELLect, ICN Biomedicals). The tubes were kept in a growth chamber (16 h light, 120 $\mu E\ s^{-1}\ m^{-2}$, 31°C; 8 h dark, 28°C). Plants were inoculated by adding 5 ml of inoculum into each test tube, when most the tomato seedlings had reached the first-leaf stage, i.e., approximately 2 weeks after germination.

Tomato plants were also grown in 8-cm-diameter peat pots containing friable horticultural humus, under the same growth chamber conditions. When plants have reached second-leaf stage, approximately 2 weeks after planting, they were inoculated by soaking the pots in a bacterial inoculum for 30 min.

Microscopic methods.

Light microscopy.

Light microsopy was performed on whole roots, on root sections, and on slices of plant axe.

Whole roots of seedlings were processed, 6, 12, and 24 h after inoculation and then daily over a period of 2 weeks. Roots were fixed for 2 h in a solution of 1.25% (v/v) glutaraldeyde in 0.15 M, sodium cacodylate buffer, adjusted to pH 7.2, in order to inactivate endogenous plant β-galactosidase activity (Teeri et al. 1989), then rinsed 3 times each for 15 min in the same buffer. Histochemical staining of bacterial β-galactosidase activity was performed using X-Gal (5-bromo-4-chloro-3-indolyl-β-D-galacotopyranoside) as substrate following the procedure described by Boivin et al. (1990). Whole roots were observed by bright-field microscopy using a light microscope (Vanox, Olympus).

Root sections were obtained as follows: 2- to 3-mm root segments of interest were dissected from whole roots already fixed and histochemically stained as described above. They were successively fixed again in a solution of 2.5% glutaraldehyde in 0.2 M sodium cacodylate buffer (v/v) adjusted to pH 7.2, dehydrated in an ethanol series and progressively embedded in LR White resin, medium grade (TAAB Laboratories). Polymerization was performed at 58°C during 48 h.

Embedded samples were cut with an ultramicrotome (Ultracut E, Reichert-Jung) with diamond knives. Semithin sections, 1.5 μm thick, were deposited on glass slides and observed by light microscopy either unstained or after staining with a mixture of 1% (w/v) toluidine blue and 2% (w/v) methylene blue in a 1% (w/v) aqueous solution of sodium borate (Millonig 1976).

Slices were obtained from partially wilted tomato plants cultivated in pot conditions. Ten days after inoculation, 1 cm long segments were cut off from the plant axis at the four levels described in the text. Segments of the same plant were stained for bacterial β-galactosidase activity and fixed again as described above. Each segment was then cut into 200-μm-thick transverse slices using a vibratome (Microcut H 1200, Biorad). Slices were observed by bright-field microscopy without further staining.

Electron microscopy.

Utrastructural observations were performed on ultrathin sections of embedded root segments (see above). Sections were stained with uranyl acetate 2.5% (w/v) in 50% ethanol then with lead citrate (Venable and Coggesthal 1995) and observed with a transmission electron microscope (EM 600, Hitachi) operating at 75 kV.

ACKNOWLEDGMENTS

We are grateful to C. Boucher for providing us with the strain GMI1485, to C. Etchebar for construction of the strain GMI2550, and to M. Arlat for his help in enzyme activity assays. We thank many colleagues from our laboratory, but particularly G. Truchet, for stimulating discussions and valuable criticism of the manuscript and C. Gough and N. Grimsley for reviewing the manuscript.

LITERATURE CITED

Agrios, G. N. 1988. Plant diseases caused by prokaryotes. Pages 510-609 in: Plant Pathology. 3rd ed. Academic Press, Inc., San Diego.

Allen, C., Simon, L., Atkinson, M., and Sequeira, L. 1993. Analysis of polygalacturonase as a component of bacterial wilt disease. Pages 238-244 in: Bacterial Wilt. Proc. Int. Conf. Taiwan. 1992. G. L. Hartman and A. C. Hayward, eds. ACIAR Proc. No. 45.

Arlat, M. 1989. Contribution à l'étude des déterminants génétiques du pouvoir phytopathogène de *Pseudomonas solanacearum.* Ph.D. thesis. Paul Sabatier University, Toulouse, France.

Arlat, M., Gough, C. L. Zischek, C., Barberis, P. A., Trigalet, A., and Boucher, C. A. 1992. Transcriptional organization and expression of the large *hrp* gene cluster of *Pseudomonas solanacearum.* Mol. Plant-Microbe Interact.5:187-193.

Ardourel, M., Demont, N., Debellé, F., Maillet, F., de Billy, F., Promé, J.-C., Dénarié, J., and Truchet, G. 1994. *Rhizobium meliloti* lipooligosaccharide nodulation factors: Differential structural requirements for bacterial entry into target root hair cells and induction of plant symbiotic developmental responses. Plant Cell 6:1357-1374.

Beckman, C. H. 1987. The Nature of Wilt Diseases of Plants. American Phytopathological Society, St. Paul, Minnesota.

Bishop, C. D., and Cooper, R. M. 1983. An ultrastructural study of vascular colonization in three vascular wilt diseases. I. Colonization of susceptible cultivars. Physiol. Plant Pathol. 23:323-343.

Boivin, C., Camut, S., Malpica, C. A., Truchet, G., and Rosenberg, C. 1990. *Rhizobium meliloti* genes encoding catabolism of Trigonelline are induced under symbiotic conditions. Plant Cell 2:1157-1170.

Boucher, C. A., Barberis, P. A., Trigalet, A. P., and Demery, D. A. 1985. Transposon mutagenesis of *Pseudomonas solanacearum:* Isolation of Tn5-induced avirulent mutants. J. Gen. Microbiol. 131:2449-2457.

Boucher, C., Martinel, A., Barberis, P., Alloing, G., and Zischek, C. 1986. Virulence genes are carried by a megaplasmid of the plant pathogen *Pseudomonas solanacearum.* Mol. Gen. Genet. 205:270-275.

Boucher, C. A., Van Gijsegem, F., Barberis, P. A., Arlat, M., and Zischek, C. 1987. *Pseudomonas solanacearum* genes controlling both pathogenicity on tomato and hypersensitivity on tobacco are clustered. J. Bacteriol. 169:5626-5632.

Boucher, C. A., Gough, C. L., and Arlat, M. 1992. Molecular genetics of pathogenicity determinants of *Pseudomonas solanacearum* with special emphasis on *hrp* genes. Annu. Rev. Phytopathol. 30:443-461.

Brumbley, S. M., and Denny, T. P. 1990. Cloning of wild-type *Pseudomonas solanacearum phcA,* a gene that when mutated alters expression of multiple traits that contribute to virulence. J. Bacteriol. 172:5677-5685.

Buddenhagen, I. W. 1986. Bacterial wilt revisited. Pages 126-143 in: Bacterial Wilt in Asia and South Pacific. Proc. Int. Workshop PCARRD, Los Baños, Philippines. Persley, G. J., ed.

Buddenhagen, I., and Kelman, A. 1964. Biological and physiological aspects of bacterial wilt caused by *Pseudomonas solanacearum.* Annu. Rev. Phytopathol. 2:203-230.

Couteaudier, Y., Daboussi, M.-J., Eparvier, A., Langin, T., and Orcival, J. 1993. The GUS fusion system (*Escherichia coli* β-D-glucuronidase gene), a useful tool in studies of root colonization by *Fusarium oxysporum.* Appl. Environ. Microbiol. 59:1767-1773.

Denny, T. P., Carney, B. F., and Schell, M. A. 1990. Inactivation of multiple virulence genes reduces the ability of *Pseudomonas solanacearum* to cause wilt symptoms. Mol. Plant-Microbe Interact. 3:293-300.

Denny, T. P., and Baek, S.-R. 1991. Genetic evidence that extracellular polysaccharide is a virulence factor of *Pseudomonas solanacearum.* Mol. Plant-Microbe Interact. 4:198-206.

Drigues, P., Demery-Lafforgue, D., Trigalet, A., Dupin, P., Samain, D., and Asselineau, J. 1985. Comparative studies of lipopolysaccharide and exopolysaccharide from virulent strain of *Pseudomonas solanacearum* and from three avirulent mutants. J. Bacteriol.162:504-509.

Duvick, J. P., and Sequeira, L. 1984. Interaction of *Pseudomonas solanacearum* lipopolysaccharide and extracellular polysaccharide with agglutinin from potato tubers. Appl. Environ. Microbiol. 48:192-198.

Forster, R. C. 1986. The ultrastructure of the rhizoplane and rhizosphere. Annu. Rev. Phytopathol. 24:211-234.

Hadas, R., and Okun, Y. 1987. Effect of *Azospirillum brasilense* inoculation on root morphology and respiration in tomato seedlings. Biol. Fertil. Soils. 5:241-247.

Hayward, A. C. 1991. Biology and epidemiology of bacterial wilt caused by *Pseudomonas solanacearum.* Annu. Rev. Phytopathol. 29:65-87.

Kang, Y., Huang, J., Mao, G., He, L., and Schell, M. A. 1994. Dramatically reduced virulence of mutants of *Pseudomonas solanacearum* defective in export of extracellular proteins across the outer membrane. Mol. Plant-Microbe Interact. 7:370-377.

Kelman, A. 1953. Host-parasite relations. Pages 95-104 in: The Bacterial Wilt Caused by *Pseudomonas solanacearum.* Tech. Bull. No. 99. A N.C. State College Publication. North Carolina Agric. Exp. Stn.

Millonig, G. 1976. Page 58 in: Laboratory Manual of Biological Microscopy. M. Saviolo, ed. Vercelli, Italy.

Message, B., Boisard, P., Pitrat, M., Schmit, J., and Boucher, C. 1978. A new class of fluidal avirulent mutants of *Pseudomonas solanacearum* unable to induce a hypersensitive reaction. Pages 823-833 in: Proc. 4th Int. Conf. Plant Pathol. Bacteriol. INRA. Angers, France.

Orgambide, G., Montrozier, H., Servin, P., Trigalet-Demery, D., and Trigalet, A. 1991. High heterogeneity of the exopolysaccharides of *Pseudomonas solanacearum* strain GMI1000 and the complete structure of the major polysaccharide. J. Biol. Chem. 266:8312-8321.

Petrolini, B., Quaroni, S., and Saracchi, M. 1986. Scanning electron microscopy investigations on the relationships between bacteria and plant tissues. II. Investigations on initial processes of *Pseudomonas solanacearum* pathogenesis. Riv. Pat. Veg. S IV, 22:100-105.

Pontier, D., Godiard, L., Marco, Y., and Roby, D. 1994. *hsr*203J, a tobacco gene whose activation is rapid, highly localized and specific for incompatible plant/pathogen interactions. Plant J. 5:507-521.

Robb, J., Powell, D. A., and Street, P. F. S. 1987. Vascular coating: A barrier to colonization by the pathogen in *Verticillium* wilt of tomato. Can. J. Bot. 67:600-607.

Rovira, A. D. 1973. Zones of exudation along plant roots and spatial distribution of microorganisms in the rhizosphere. Pestic. Sci. 4: 361-366.

Schell, M. A. 1987. Purification and characterization of an endoglucanase from *Pseudomonas solanacearum.* Appl. Environ. Microbiol. 53:2237-2241.

Schell, M. A., Roberts, D. P., and Denny, T. P. 1988. Cloning of the *pglA* gene of *Pseudomonas solanacearum* and its involvement in phytopathogenicity. J. Bacteriol. 170:4501-4508.

Schmit, J. 1978. Microscopic study of early stages of infection by *Pseudomonas solanacearum* E. F. S. on "in vitro" grown seedlings. Pages 841-856 in: Proc. 4th Int. Conf. Plant Pathol. Bacteriol. INRA. Angers, France.

Sequeira, L. 1993. Bacterial wilt: Past, present, and future. Pages 12-21 in: Bacterial Wilt. Proc. Int. Conf. Taiwan. 1992. G. L. Hartman and A. C. Hayward, eds. ACIAR Proc. No. 45.

Shi, J., Mueller, C., and Beckman, C. H. 1992. Vessel occlusion and secretory activities of vessel contact cells in resistant or susceptible cotton plants infected with *Fusarium oxysporum* f. sp. *vasinfectum.* Physiol. Mol. Plant Pathol. 40:133-147.

Simon, R., Quandt, J., and Klipp, W. 1989. New derivatives of transposon Tn*5* suitable for mobilization of replicons, generation of operon fusions and induction of genes of Gram-negative bacteria. Gene 80:161-169.

Street, P. F. S., Robb, J., and Ellis, B. E. 1986. Secrection of vascular coating components by xylem parenchyma cells of tomatoes infected with *Verticillium albo-atrum.* Protoplasma 132:1-11.

Talboys, P. W. 1964. A concept of the host-parasite relationship in *Verticillium* wilt diseases. Nature 202:361-364.

Teeri, T. H., Lehväslaiho, H., Franck, M., Uotila, J., Heino, P., Palva, E. T., Van Montagu, M., and Herrera-Estrella, L. 1989. Gene fusions to *lacZ* reveal new expression patterns of chimeric genes in transgenic plants. EMBO J. 8:343-350.

Trigalet, A., and Trigalet-Demery, D. 1990. Use of avirulent mutants of *Pseudomonas solancearum* for the biological control of bacterial wilt of tomato plants. Physiol. Mol. Plant Pathol. 36:27-38.

Vasse, J., de Billy, F., and Truchet, G. 1993. Abortion of infection during the *Rhizobium meliloti*–alfalfa symbiotic interaction is accompanied by a hypersensitive reaction. Plant J. 4:555-566.

Venable, J. H., and Coggeshal, R. 1965. A simplified lead citrate stain for use in electron microscopy. J. Cell Biol. 25:407-414.

Wallis, F. M. 1977. Ultrastructural histopathology of tomato plants infected with *Corynebacterium michiganense.* Physiol. Plant Pathol. 11:333-342.

Wallis, F. M., Rijkenberg, F. H. J., Joubert, M., and Martin, M. M. 1973. Ultrastructural histopathology of cabbage leaves infected with *Xanthomonas campestris.* Physiol. Plant Pathol. 3:371-378.

Wallis, F. M., and Truter, S. J. 1978. Histopathology of tomato plants infected with *Pseudomonas solanacearum,* with emphasis on ultrastructure. Physiol. Plant Pathol. 13:307-317.

Young, D. H., and Sequeira, L. Binding of *Pseudomonas solanacearum* fimbriae to tobacco leaf cell walls and its inhibition by extracellular polysaccharides. Physiol. Mol. Plant Pathol. 28:393-402.

Yu, P. T., Stolzy, H., and Letey, J. 1969. Survival of plants under prolonged flooded conditions. Agron. J. 61:844-847.